

## Feedback mechanism in network dynamics with preferential flow

H. Fan,<sup>1,\*</sup> Z. Wang,<sup>2,†</sup> L. Chen,<sup>1,3</sup> and K. Aihara<sup>1,3</sup>

<sup>1</sup>*Department of Mathematical Informatics, Graduate School of Information Science and Technology, The University of Tokyo, 7-3-1 Hongo, Bunkyo-Ku, Tokyo 113-8656, Japan*

<sup>2</sup>*College of Information Science and Technology, Donghua University, Shanghai 200051, China*

<sup>3</sup>*ERATO Aihara Complexity Modelling Project, JST, 45-18 Oyama, Shibuya-ku, Tokyo 151-0065, Japan*

(Received 7 July 2008; revised manuscript received 22 December 2008; published 20 February 2009; publisher error corrected 25 February 2009)

We study complex systems or networks in which each node holds an internal dynamics and interacts with other nodes through some kinds of topologies. Collective behavior with dynamical fluctuations is analyzed in complex systems. The dynamical fluctuations of a node can be divided into two parts: one is the internal dynamical fluctuation of the node and the other is the external dynamical fluctuation caused by other nodes. Based on a theoretical analysis, a hidden feedback mechanism is identified in complex systems, which is illustrated in a macroeconomic network and in a city-population network. Furthermore, we study the effect of the topology of the networks on the feedback mechanism. The feedback mechanism is preserved for hub nodes in the networks with a scale-free topology as well as in the networks with an evolving topology. By the hidden feedback mechanism, the observation data can be utilized to judge directly whether the system of each node is with positive feedback or with negative feedback even without knowing its dynamical model.

DOI: [10.1103/PhysRevE.79.026107](https://doi.org/10.1103/PhysRevE.79.026107)

PACS number(s): 89.75.Hc, 89.65.-s

### I. INTRODUCTION

Complex systems pervade all of science, from neurobiology to statistical physics [1]. Many real-world networks can be considered as complex systems where the dynamics is determined by the interaction of a large number of nodes through some kinds of topologies with each node holding an internal dynamical rule. For example, for a macroeconomic network, a node can be viewed as a country; the interaction of nodes is the trade between the countries, and the internal dynamics of a country is the dynamics of GDP in the country. Taking a city-population network as another example, a node can be a city; the interaction of nodes is the population transfer between the cities, and the internal dynamics of the city reflects the change of the population with time. Collective behavior emerges in such complex systems. For instance, the behavior of synchronization has been found in various complex networks, where the dynamics of each node is an identical or nonidentical limit cycle, and the interaction of nodes is under some kinds of topologies [2–5]. Another kind of collective behavior is the fluctuation dynamics, which arises when complex systems are exposed to various kinds of shocks. In the macroeconomic network, every country is exposed to the shocks such as the variation of money policy and fiscal policy. For the transport and internet system, the traffic increases on highways during peak hours and surges in the number of internet users during working hours [6]. Generally, the dynamics of each node in such complex systems mentioned above is determined by two factors: (1) the internal dynamics of the node and (2) the external dynamics of the node that is decided by the interactive coupling with other nodes. Accordingly, the fluctuation dynamics of

complex systems includes the internal dynamical fluctuation and the external dynamical fluctuation for each node.

There are many studies focusing on the statistical fluctuation behavior of the time series of complex systems. A general feature related to the scaling properties of the statistical fluctuation behavior is called the Taylor's law, which has been found in many complex systems such as ecology, life sciences, physics, and economy [7,8]. Recently, the same relationship is explored on complex networks [6,9–12]. Most of the models that try to explain the statistical fluctuation behavior in complex systems to date assume that the dynamics of the nodes or units is stationary, whose activity can be formalized by an additive quantity. As the dynamics of many real-world complex systems is determined by the interaction of a large number of nodes with each node holding an internal dynamical rule, the scaling properties of the statistical fluctuation behavior is not enough to identify the underlying fluctuation dynamics of complex systems [8].

In this paper, we study the fluctuation dynamics of complex systems, where the dynamics of each node is decided by the internal dynamics, external dynamics, and shocks. Specifically, we aim at answering the questions: whether the external dynamical fluctuation strengthens or weakens the internal dynamical fluctuation of a node; under what conditions, the dynamics of a node is dominated only by its internal dynamics. These questions motivate the research in this paper. First, a model is proposed in Sec. II and a feedback mechanism is derived in the model. In Sec. III, the feedback mechanism is illustrated. The illustration of the feedback mechanism in a macroeconomic network is presented in Sec. III A and that in a city-population network is presented in Sec. III B, respectively. The effect of the topology on the feedback mechanism is shown in Sec. IV. In Sec. V, the real-world data are used to illustrate the feedback mechanism. Finally, summary and discussions will be given in Sec. VI.

\*hongfan@sat.t.u-tokyo.ac.jp

†wangzj@dhu.edu.cn

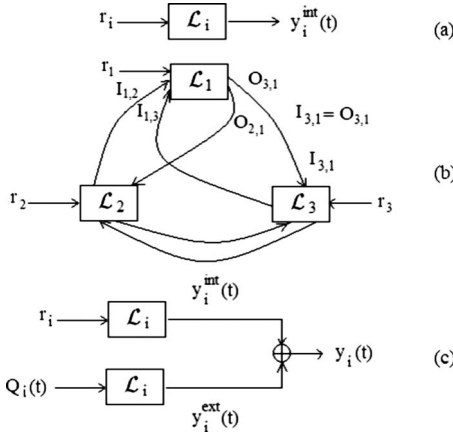


FIG. 1. A network. (a) The internal dynamical rule of node  $i$ , (b) the network with three nodes, and (c) the summation of the internal dynamics and external dynamics.

## II. MODEL

Let us consider  $N$  different linear systems denoted by  $\mathcal{L}_i$  with an input  $r_i$  in Fig. 1(a), where each system is assumed to be asymptotically stable. By interacting with each other through some kinds of topologies, these  $N$  linear systems constitute a complex system, where each node represents one linear system [23]. Figure 1(b) shows such a complex network with three nodes. Each node [e.g., see node 1 in Fig. 1(b)] has input flux and output flux. As  $\mathcal{L}_i$  is a linear system, we divide the dynamics of a node in the network into two parts [13] [see Fig. 1(c)]:

$$y_i(t) = y_i^{\text{int}}(t) + y_i^{\text{ext}}(t), \quad (1)$$

where  $y_i(t)$  is the state of the node in the network. For a macroeconomic system,  $y_i(t)$  is the GDP of country  $i$  at time  $t$ ; for a city-population system,  $y_i(t)$  is the population in city  $i$  at time  $t$ .  $y_i^{\text{int}}(t)$  is the internal dynamics of system  $\mathcal{L}_i$  with input  $r_i$ . Namely,  $y_i^{\text{int}}(t)$  is the dynamics of system  $\mathcal{L}_i$  without interacting with any other systems or nodes [see Fig. 1(a)].  $y_i^{\text{ext}}(t)$  represents the effect of external net flux dynamics  $Q_i(t) = \sum_{j=1}^N I_{i,j}(t) - \sum_{j=1}^N O_{j,i}(t)$  with  $I_{i,j}(t)$  being the input flux of node  $i$  from node  $j$  and  $O_{j,i}(t)$  being the output flux of node  $i$  to node  $j$ . It is worth noting that both  $I_{i,j}$  and  $O_{i,j}$  represent the amount of flux from nodes  $j$  to  $i$ , i.e.,  $I_{i,j} = O_{j,i}$  [see Fig. 1(b)].

As shown in Figs. 2(a) and 2(b), the network at an equilibrium point implies that the internal dynamics, the external dynamics, and the net flux are in equilibrium  $y_i^{\text{int}*}$ ,  $y_i^{\text{ext}*}$ , and  $Q_i^*$ , respectively. However, internal linear system  $\mathcal{L}_i$  ceaselessly suffers from shocks or noises [see Fig. 2(c)], yielding the internal fluctuation  $\Delta y_i^{\text{int}}(t)$ . In addition to shocks, the system  $\mathcal{L}_i$  in the network suffers from the net flux fluctuation  $R_i(t) = Q_i(t) - Q_i^*$  as well [see Fig. 2(d)], which yields the external fluctuation  $\Delta y_i^{\text{ext}}(t)$ . Then the network fluctuation of the system  $\mathcal{L}_i$  is the summation of the internal and external fluctuations  $\Delta y_i(t) = \Delta y_i^{\text{int}}(t) + \Delta y_i^{\text{ext}}(t)$  [see Fig. 2(d)]. The effect of the shocks is characterized by a stochastic variable  $\phi_i(t)$  with the normal distribution in the present paper  $\phi_i(t) = \xi_i(t) \alpha_i(t)$  with  $\xi_i(t) \sim N(0, 1)$  and  $\alpha_i(t) > 0$ . Herein, an im-

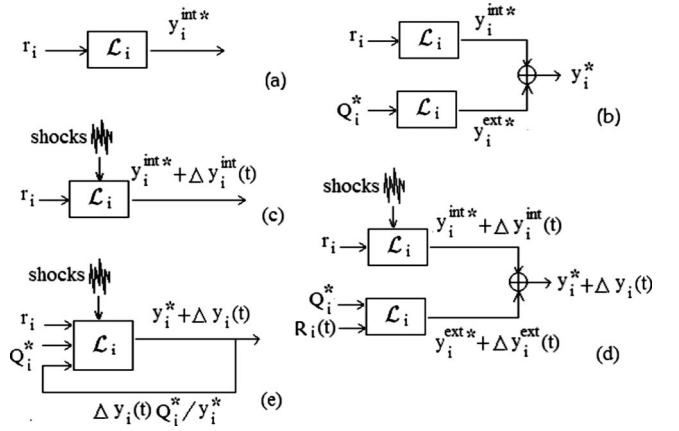


FIG. 2. Internal and external dynamical fluctuations. (a), (b) The equilibrium point of the internal and external dynamics. (c), (d) The internal and external fluctuations, and (e) the feedback mechanism.

portant question emerges, i.e., does the external fluctuation  $\Delta y_i^{\text{ext}}(t)$  strengthen or weaken the internal fluctuation  $\Delta y_i^{\text{int}}(t)$ ?

To address this problem, we first calculate the net flux fluctuation  $R_i(t)$ . Assume that the larger  $y_i(t)$  is, the larger input flux and output flux of node  $i$  at time step  $t$  are. This assumption is consistent with the case  $\gamma < 1$  in Ref. [14] for an internet system. It is also plausible for some other real-world networks. For example, in the macroeconomic network, the larger GDP one country has, the larger imports and exports the country has. For the city-population network, the higher population one city has, the larger population transfer the city has. The same phenomena can also be found in the traffic system and the river network system. Here, we name such phenomena as preferential flow. Hence, the output flux of node  $j$  at time step  $t$  is linearly proportional to the state of the node at time step  $t-1$ , i.e.,  $\sum_{i=1}^N O_{i,j}(t) = k_j y_j(t-1)$  with  $0 < k_j < 1$ ; the flux from node  $j$  to  $i$  is also linearly proportional to the state of the node  $i$ , i.e.,  $O_{i,j}(t) = s_{i,j}(t) k_j y_j(t-1)$  with the following  $s_{i,j}(t)$ :

$$s_{i,j}(t) = \frac{w_{i,j} y_i(t-1)}{\sum_{l=1}^N w_{l,j} y_l(t-1)}, \quad (2)$$

where  $0 \leq w_{l,j} \leq 1$  represents a weighted topological structure of the network.  $w_{l,j} = 0$  implies no flux from node  $j$  to node  $l$ . We assume  $w_{l,l} = 0$  in the present paper. Thus,

$$Q_i(t) = \sum_{j=1}^N s_{i,j}(t) k_j y_j(t-1) - k_i y_i(t-1). \quad (3)$$

Equation (3) ensures the flux conservation because  $\sum_{i=1}^N \frac{w_{i,j} y_i(t-1)}{\sum_{l=1}^N w_{l,j} y_l(t-1)} k_j y_j(t-1) = k_j y_j(t-1)$ .

The steady net flux  $Q_i^*$  can be calculated by

$$Q_i^* = \sum_{j=1}^N \frac{w_{i,j} y_j^*}{\sum_{l=1}^N w_{l,j} y_l^*} k_j y_j^* - k_i y_i^*. \quad (4)$$

If  $Q_i^* > 0$ , clearly node  $i$  has a positive net flux balance. On the other hand,  $Q_i^* < 0$  means a negative net flux balance for node  $i$ .

The general form of the internal dynamics of node  $i$ , the linear system  $\mathcal{L}_i$ , can be given as

$$y_i^{\text{int}}(t) = \sum_{j=1}^{L_i} b_{i,j} y_i^{\text{int}}(t-j) + \sum_{j=0}^{P_i} g_{i,j} u_i(t-j), \quad (5)$$

where  $u_i(t)$  is the input of the system,  $L_i$  and  $P_i$  are constants,  $L_i$  is the order of the system, and  $b$  and  $g$  are the parameters of the system. Figure 1(a) shows the case that  $\mathcal{L}_i$  has a constant input  $r_i$ . Then the network dynamics with preferential flow for node  $i$  [see Fig. 2(d)] can be described by

$$y_i(t) = \sum_{j=1}^{L_i} b_{i,j} y_i(t-j) + \sum_{j=0}^{P_i} g_{i,j} [Q_i(t-j) + \phi_i(t-j) + r_i], \quad (6)$$

where  $Q_i(t) = R_i(t) + Q_i^*$ , which is defined by Eqs. (2) and (3).

If  $N$  is sufficiently large, then the relationship between  $R_i(t+1)$  and  $\Delta y_i(t)$  can be derived through a nontrivial manipulation (see Appendix A):

$$R_i(t+1) = \Delta y_i(t) Q_i^* / y_i^*. \quad (7)$$

Equation (7) implies a hidden feedback mechanism. According to Eq. (7), Fig. 2(d) can be reorganized as Fig. 2(e), which actually describes the hidden feedback mechanism: (1) if node  $i$  has a positive net flux balance, then the sign of  $R_i(t+1)$  is identical to that of  $\Delta y_i(t)$ , namely,  $Q_i^* > 0 \Rightarrow \text{sgn}[R_i(t+1)] = \text{sgn}[\Delta y_i(t)]$ , resulting in a positive feedback for node  $i$ ; (2) if node  $i$  has a negative net flux balance, then the sign of  $R_i(t+1)$  is opposite to that of  $\Delta y_i(t)$ , namely,  $Q_i^* < 0 \Rightarrow \text{sgn}[R_i(t+1)] = -\text{sgn}[\Delta y_i(t)]$ , yielding a negative feedback for node  $i$ ; (3) if  $Q_i^* = 0$ , the fluctuation dynamics of nodes is decided only by their internal fluctuation dynamics.

According to the control theory [15], suppression of disturbances (shocks) is an internal mechanism for a negative feedback system. A positive feedback system, on the other hand, generally suffers more from fluctuations. Hence, we have the major results: if  $Q_i^* > 0$ , then the external dynamical fluctuation strengthens the internal dynamical fluctuation due to the positive feedback, whereas if  $Q_i^* < 0$ , the external dynamical fluctuation weakens the internal dynamical fluctuation due to the negative feedback. If  $Q_i^* = 0$ , the external dynamical fluctuation has no effect on the internal dynamical fluctuation.

### III. ILLUSTRATION OF THE FEEDBACK MECHANISM

#### A. Illustration of the feedback mechanism in a macroeconomic network

We next illustrate the derived feedback mechanism in a macroeconomic network. The internal macroeconomic dynamics of country  $i$  can be described by

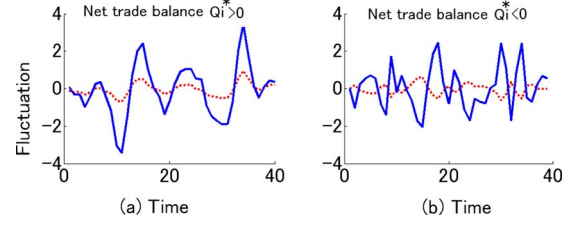


FIG. 3. (Color online) Demonstration of the hidden feedback mechanism by the evolution of fluctuation of  $y_i(t) - y_i^*$  (blue solid line) and feedback input  $R_i(t)$  (red dotted line) in two countries. (a) The sign of  $y_i(t) - y_i^*$  is identical to that of  $R_i(t)$ , implying a positive feedback effect, and (b) the sign of  $y_i(t) - y_i^*$  is opposite to that of  $R_i(t)$ , implying a negative feedback effect. The parameter values and the initial states of  $y_i$  in the simulation are set as follows:  $N=150$ ;  $k_i, c_i, v_i, T_i, w_{i,j}, z_i, y_i(0)$ , and  $y_i(1)$  are uniformly distributed in the interval  $(0,0.8)$ ,  $(0.1,0.7)$ ,  $(0,0.9)$ ,  $(0.3,1)$ ,  $[0,1]$ ,  $(0,50)$ ,  $(50,150)$ , and  $(50,150)$ , respectively.  $\phi_i(t) = \xi_i(t) \alpha_i(t) = 0.01 \xi_i(t) y_i(t-1)$ .

$$y_i^{\text{int}}(t) = (c_i + v_i c_i) y_i^{\text{int}}(t-1) - v_i c_i y_i^{\text{int}}(t-2) + z_i, \quad (8)$$

where  $c_i, v_i, z_i$  are macroeconomic parameters [16].  $N$  countries interact with each other through trade links, and thereby constitute a macroeconomic network

$$y_i(t) = (c_i + v_i c_i) y_i(t-1) - v_i c_i y_i(t-2) + z_i + Q_i(t) + \phi_i(t),$$

$$Q_i(t) = \sum_{j=1}^N \frac{w_{j,i} T_j y_j(t-1) k_j y_j(t-1)}{\sum_{l=1}^N w_{j,l} T_l y_l(t-1)} - k_i y_i(t-1), \quad (9)$$

where  $y_i(t)$  represents the GDP of country  $i$  at time step  $t$ ;  $\phi_i(t)$  is the effect of shocks;  $\sum_{j=1}^N \frac{w_{j,i} T_j y_j(t-1) k_j y_j(t-1)}{\sum_{l=1}^N w_{j,l} T_l y_l(t-1)}$  represents exports and  $k_i y_i(t-1)$  denotes imports of country  $i$ ;  $T_i$  is a parameter [17];  $w_{i,j}$  models the trade barrier between two countries.  $w_{j,i} = 0$  means no trade flux from countries  $i$  to  $j$ .

The simulation results in Fig. 3(a) reveal that for the country that gains from a positive net trade balance, the sign of  $R_i(t)$  is identical to that of fluctuation  $y_i(t) - y_i^*$ , which implies that the macroeconomic system of the country becomes a positive feedback system. Thus the macroeconomic system of the country fluctuates more than its corresponding internal macroeconomic system due to the feedback effect. On the other hand, for the country that suffers from a negative net trade balance, the sign of  $R_i(t)$  is opposite to that of  $y_i(t) - y_i^*$  [see Fig. 3(b)]. Thus, the macroeconomic system of the country becomes a negative feedback system and experiences less fluctuations than its internal macroeconomic system. Figure 4 illustrates the simulation results obtained from the comparison of the strength of fluctuations in the macroeconomic systems of countries and their corresponding internal macroeconomic systems, which are defined by  $\sum_{t=0}^{200} |y_i(t) - y_i^*| / y_i^*$  and  $\sum_{t=0}^{200} |y_i^{\text{int}}(t) - y_i^{\text{int}*}| / y_i^{\text{int}*}$ , respectively. Clearly Fig. 4 agrees with the derived feedback mechanism well.

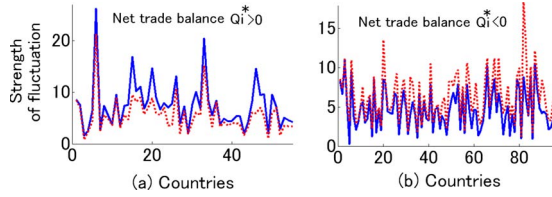


FIG. 4. (Color online) Comparison of the strength of fluctuations in the systems of countries (blue solid line) and their internal dynamical systems (red dotted line). (a) The systems of the countries show more fluctuations than their internal dynamical systems in the case of the positive net trade balance due to the positive feedback. (b) The systems of the countries show less fluctuations than their internal dynamical systems in the case of the negative net trade balance due to the negative feedback. The parameter values are set the same as those of Fig. 3.

### B. Illustration of the feedback mechanism in a city-population network

The theoretical results on the feedback mechanism require a linear system for the internal dynamics of nodes. However, the internal dynamics of nodes for many real-world systems is generated by nonlinear systems. For such systems, the feedback mechanism still holds around the equilibrium point. We next show the fact numerically by a city-population network. The internal population dynamics of a city is generated by the logistic map [24]:  $y_i^{\text{int}}(t) = a_i y_i^{\text{int}}(t-1)[1 - y_i^{\text{int}}(t-1)]$ . Then, the city-population network can be described by

$$y_i(t) = a_i y_i(t-1)[1 - y_i(t-1)] + Q_i(t) + \phi_i(t),$$

$$Q_i(t) = \sum_{j=1}^N \frac{w_{i,j} y_j(t-1) k_j y_j(t-1)}{\sum_{l=1}^N w_{l,j} y_l(t-1)} - k_i y_i(t-1), \quad (10)$$

where  $y_i(t)$  represents the population of city  $i$  at time step  $t$ ;  $\phi_i(t)$  is the effect of shocks;  $k_i y_i(t-1)$  denotes the population moving out city  $i$  and  $\sum_{j=1}^N \frac{w_{i,j} y_j(t-1) k_j y_j(t-1)}{\sum_{l=1}^N w_{l,j} y_l(t-1)}$  represents the population moving in city  $i$ ; and  $w_{i,j}$  is the topology of the network. Figure 5 shows the feedback mechanism with the results similar to those in Figs. 3 and 4.

## IV. EFFECT OF THE TOPOLOGY ON THE FEEDBACK MECHANISM

### A. Feedback mechanism in a scale-free network

Many real-world networks are found to be scale-free, implying that the degree distribution of the networks follows the power law [18–20]. Large degree nodes or hub nodes play essential roles in the scale-free networks. To verify the feedback mechanism in the scale-free networks, a scale-free undirected network with exponent 1.8 is constructed. The network is composed of  $N$  nodes. An edge between nodes  $i$  and  $j$ ,  $l_{i,j}$ , means a route for the output of node  $i$  flowing to node  $j$  and a route for the output of node  $j$  flowing to node  $i$  in the context. We then define  $0 < w_{i,j} < 1$  to describe the barrier for the output of node  $j$  flowing to node  $i$ , as well as

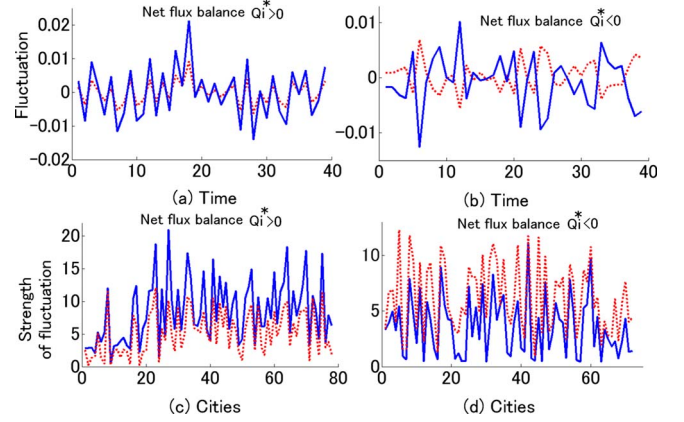


FIG. 5. (Color online) Feedback mechanism in a city-population network. (a) The sign of the fluctuation of population  $y_i(t) - y_i^*$  (blue solid line) is identical to that of the feedback input  $R_i(t)$  (red dotted line) in a city with  $Q_i^* > 0$ , (b) the sign of the fluctuation of population (blue solid line) is opposite to that of the feedback input (red dotted line) in a city with  $Q_i^* < 0$ , (c) the systems of the cities (blue solid line) show more fluctuations than their internal dynamical systems (red dotted line) in the case of  $Q_i^* > 0$ , and (d) the systems of the cities (blue solid line) show less fluctuations than their internal dynamical systems (red dotted line) in the case of  $Q_i^* < 0$ . The parameter values in the simulation are set as follows:  $N=150$ ;  $a_i$ ,  $k_i$ , and  $w_{i,j}$  are uniformly distributed in the interval  $(2.0, 2.6)$ ,  $(0, 0.6)$ , and  $[0, 1]$ , respectively.  $\phi_i(t) = \xi_i(t) \alpha_i(t) = 0.01 \xi_i(t) y_i(t-1)$ . For a delicate comparison,  $2R_i(t)$  is plotted in panels (a) and (b).

the  $0 < w_{j,i} < 1$  to describe the barrier for the output of node  $i$  flowing to node  $j$ . If there is no edge between nodes  $i$  and  $j$ , then  $w_{i,j} = w_{j,i} = 0$ . For a node  $i$  with a large degree, there are a large number of nodes that connect to it, implying that there are a large number of routes for the the output flux of node  $i$ , which suggests a large value of  $k_i$ . Therefore, we assume that  $k_i$  is uniformly distributed in the interval  $(0, d_i/N)$ , where  $d_i$  is the degree of node  $i$ . The dynamical rule of each node and the parameter setting are the same as those in Sec. III A. The steady net flux  $Q_i^*$  and the feedback signal  $R_i(t)$  are calculated. Figure 6(a) shows the evolution of  $R_i(t)$  and  $y_i(t) - y_i^*$  of a large degree node (hub) with a negative net balance flux. Figure 6(a) confirms the feedback mechanism within large degree nodes (hubs) in the scale-free network since  $y_i(t) - y_i^*$  and  $R_i(t)$  are in antiphase. The feedback mechanism also holds in networks with other topologies such as a network with a Poisson degree distribution and a network with an exponential degree distribution.

The derivation of the feedback mechanism needs a sufficiently large number of nodes and completely connected topology, i.e., needs sufficiently large degrees of all the nodes in the network. A node with a small degree in a scale-free network may violate the feedback mechanism. For example, the fluctuation of a node with only one link may be dominated by a large degree node that it links to, rather than holding the feedback mechanism. If there are too many such small degree nodes in the network, the feedback mechanism in large degree nodes may also be destroyed.

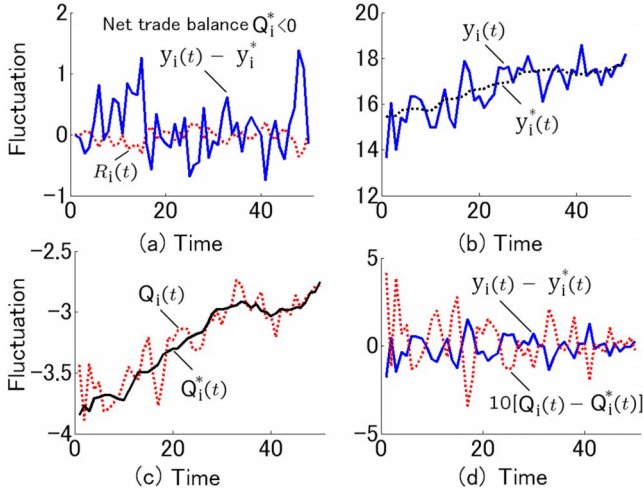


FIG. 6. (Color online) The effect of the topology of the network on the feedback mechanism. The result in (a) is obtained in a scale-free network whose topology does not change with time.  $y_i(t) - y_i^*$  (blue solid line) and  $R_i(t)$  (red dotted line) are in antiphase for a large degree node with  $Q_i^* < 0$ , implying that the mechanism is preserved for the large degree nodes in the scale-free network. The results in (b), (c), and (d) are obtained in a scale-free network with an evolving topology. The initial topology is the same as that in (a). (b) Shows the fluctuation of  $y_i(t)$  (blue solid line) around  $y_i^*(t)$  (black dotted line), (c) shows the fluctuation of  $Q_i(t)$  (red dotted line) around  $Q_i^*(t)$  (black solid line), and (d) shows that  $y_i(t) - y_i^*(t)$  (blue solid line) is in antiphase with  $10R_i(t) = 10[Q_i(t) - Q_i^*(t)]$  (red dotted line). The parameter values in the simulations are set as follows:  $N=1000$ ,  $k_i$  is uniformly distributed in the interval  $(0, d_i/N)$ , other parameters are set the same as that in Fig. 3. In panels (b)–(d), only 50 data points are plotted. The simulation results from 1 to 100 000 time steps are sampled at every 2000 time steps to obtain the 50 data points.

### B. Feedback mechanism in a network with an evolving topology

A weight matrix  $W=(w_{i,j})_{N \times N}$  can be used to represent the topology of the completely connected network. The steady state and the steady net flux of node  $i$ ,  $y_i^*$ , and  $Q_i^*$ , depend on the weight matrix  $W=(w_{i,j})_{N \times N}$ . Different  $W$  causes different  $y_i^*$  and  $Q_i^*$ . We denote  $y_i^*$  and  $Q_i^*$  as  $y_i^*|_{(w_{i,j})_{N \times N}}$  and  $Q_i^*|_{(w_{i,j})_{N \times N}}$ , respectively, to specify this dependency hereon. Thus, if  $W$  changes with time, i.e., if there is a different  $W(t)$  at each time step  $t$ , there will be a corresponding steady state and steady net flux at each time step  $y_i^*(t)|_{(w_{i,j}(t))_{N \times N}}$ ,  $Q_i^*(t)|_{(w_{i,j}(t))_{N \times N}}$ , respectively.

We first confirm the feedback mechanism in a simple scenario of the topology evolution. In this scenario, the evolution of the network topology can be described by introducing a random variable with the zero mean to the weight matrix in a completely connected network. Assume that the random variable follows normal distribution (other distribution laws, such as the uniform distribution work as well),  $w_{i,j}(t) = w_{i,j}(0) + \xi_{i,j}(t)\beta_{i,j}(t)w_{i,j}(0)$  with  $t > 0$ ,  $\xi_{i,j}(t) \sim N(0, 1)$ , and  $\beta_{i,j}(t) > 0$ . We investigate the network behavior within a time window  $\tau$ , and find that  $y_i^*(t)|_{(w_{i,j}(t))_{N \times N}}$  fluctuates around

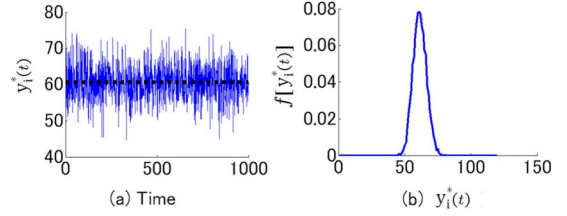


FIG. 7. (Color online) The effect of topology noise on the steady state  $y_i^*(t)|_{(w_{i,j}(t))_{N \times N}}$  of a node. (a)  $y_i^*(t)|_{(w_{i,j}(t))_{N \times N}}$  (blue solid line) fluctuates around  $y_i^*(0)|_{(w_{i,j}(0))_{N \times N}}$  (black dotted line). (b) The distribution of  $y_i^*(t)$  takes a form of normal distribution.  $f[y_i^*(t)]$  is the probability density of  $y_i^*(t)$ . The parameter values in the simulation are set as follows:  $N=10$ ,  $\beta_{i,j}(t)=0.1$ ,  $k_i$ ,  $c_i$ ,  $v_i$ ,  $T_i$ ,  $w_{i,j}(0)$ ,  $z_i$ ,  $y_i(0)$ , and  $y_i(1)$  are uniformly distributed in the interval  $(0.2, 0.8)$ ,  $(0.1, 0.8)$ ,  $(0, 0.9)$ ,  $(0.3, 1)$ ,  $[0, 1]$ ,  $(0, 50)$ , and  $(50, 150)$ , and  $(50, 150)$ , respectively.

$y_i^*(0)|_{(w_{i,j}(0))_{N \times N}}$  [see Fig. 7(a)]. We denote the means of  $y_i^*(t)$  and  $Q_i^*(t)$  within the time window  $\tau$  as  $\bar{y}_i^* = \sum_{t=0}^{\tau} y_i^*(t) / \tau$  and  $\bar{Q}_i^* = \sum_{t=0}^{\tau} Q_i^*(t) / \tau$ , respectively. Since the distribution of  $y_i^*(t)$  takes a form of normal distribution with  $y_i^*(0)$  being the mean [see Fig. 7(b)], it is natural to investigate the feedback mechanism by considering the relationship between  $y_i(t) - y_i^*(0)$  and  $Q_i(t) - Q_i^*(0)$ . Appendix B further proves that  $Q_i(t) - Q_i^*(0)$  and  $y_i(t) - y_i^*(0)$  are in in-phase (antiphase) when  $Q_i^*(0) > 0$  ( $Q_i^*(0) < 0$ ), which confirms the feedback mechanism in this case of the evolving topology.

For a general case of the topology evolution, we can utilize the average steady net flux over time window  $\tau$ ,  $\bar{Q}_i^*$  to judge the behavior of the fluctuations of the network. If  $\bar{Q}_i^* > 0$ , then node  $i$  tends to have a positive feedback signal; otherwise node  $i$  is likely to have a negative feedback signal. The evolution of the topology of a great number of real-world networks results in the rewiring dynamics [21,22]. We investigate the feedback mechanism in a network with rewiring dynamics. We consider the rewiring dynamics in the model by following six steps. Step 1: Construct and initiate the network. We start a network with the topology the same as that in Sec. IV A. Step 2: Update the states of the nodes in the network according to Eq. (9). Step 3: Select an edge among all edges randomly. Suppose that edge  $l_{i,j}$  is selected at this step. Step 4: Disconnect the selected edge  $l_{i,j}$  from the network by setting  $w_{i,j}=w_{j,i}=0$ ,  $d_i=d_i-1$ ,  $d_j=d_j-1$ ,  $k_i=k_i(1-1/d_i)$ , and  $k_j=k_j(1-1/d_j)$ . Step 5: Select two nodes in the network to add the edge disconnected from nodes  $i$  and  $j$ . The first node, node  $m$ , is selected according to the preferential attachment mechanism, by which node  $m$  is selected with a probability  $d_m / \sum_{q \in \Phi_m} d_q$ . The second node, node  $n$ , is selected among a node set  $\Phi_m$ .  $\Phi_m$  is generated by collecting all nodes that have no edge connecting with node  $m$ . Node  $n$  is selected with a probability  $d_n / \sum_{q \in \Phi_m} d_q$ . Attach the edge  $l_{i,j}$  to the two nodes  $m$  and  $n$  by letting  $w_{m,n}$  and  $w_{n,m}$  uniformly distributed in the interval  $(0,1)$ ,  $d_m=d_m+1$ ,  $d_n=d_n+1$ ,  $k_m=k_m(1+1/d_m)$ , and  $k_n=k_n(1+1/d_n)$ . Step 6: Go to step 2. Since the topology in Fig. 6(a) does not evolve with time, the steady net flux  $Q_i^*$  does not change with time. With the initial topology the same as that in Fig. 6(a),  $w_{i,j}(t)$  in Figs. 6(b)–6(d) evolves with time, hence,  $y_i^*(t)|_{(w_{i,j}(t))_{N \times N}}$  and

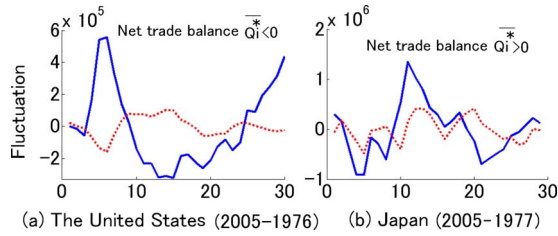


FIG. 8. (Color online) The fluctuation of GDP  $y_i(t) - y_i^*(t)$  (blue solid line) and that of the feedback signal  $R_i(t) = Q_i(t) - \bar{Q}_i^*$  (red dotted line) drawn by the real data. (a) For the U.S., the sign of feedback signal  $R_i(t)$  is opposite to that of the fluctuation of GDP. (b) For Japan, the sign of  $R_i(t)$  is nearly identical to that of the fluctuation of GDP. For a delicate comparison,  $10R_i(t)$  is plotted in panel (b).

$Q_i^*(t)|_{[w_{ij}(t)]_{N \times N}}$  evolve with time as well. Figure 6(b) shows that  $y_i(t)$  fluctuates around  $y_i^*(t)$  and Fig. 6(c) shows that  $Q_i(t)$  fluctuates around  $Q_i^*(t)$ , implying that  $y_i^*(t)$  and  $Q_i^*(t)$  are the trends of  $y_i(t)$  and  $Q_i(t)$ , respectively. By removing the trends from  $y_i(t)$  and  $Q_i(t)$ , we find in Fig. 6(d) that  $y_i(t) - y_i^*(t)$  is in antiphase with  $Q_i(t) - Q_i^*(t)$ , which agrees with the feedback mechanism since  $\bar{Q}_i^* < 0$ .

## V. ILLUSTRATION OF THE FEEDBACK MECHANISM WITH REAL-WORLD DATA

The calculation of the net flux balance  $Q_i^*$ , or  $\bar{Q}_i^* = \sum_{t=0}^{\tau} Q_i^*(t) / \tau$  for a network with an evolving topology, is needed to determine whether a system in the network is a positive or a negative feedback system. Although the exact mathematical models of many real-world complex systems are generally not available, the observation data of these systems,  $Q_i(t)$  and  $y_i(t)$ , are usually available. Since  $Q_i^*(t)$  and  $y_i^*(t)$  can be viewed as the trends of  $Q_i(t)$  and  $y_i(t)$  [note that  $Q_i(t)$  is the net flux at time step  $t$ , while  $Q_i^*(t)|_{[w_{ij}(t)]_{N \times N}}$  is the steady net flux for an evolving network at time step  $t$ ], respectively,  $\bar{Q}_i^*$  can be estimated by averaging  $Q_i(t)$  within a time window  $\tau$ , i.e.,  $\bar{Q}_i^* = \sum_{t=0}^{\tau} Q_i^*(t) / \tau \approx \sum_{t=0}^{\tau} Q_i(t) / \tau$ . For example, the observation data on the dynamics of the net trade  $Q_i(t)$  and GDP  $y_i(t)$  for each country during the period between 1976 and 2005 are available [25]. We first get  $Q_i^*(t)$  and  $y_i^*(t)$  by estimating the trends of the net trade  $Q_i(t)$  and GDP  $y_i(t)$ , respectively. Then we calculate  $\bar{Q}_i^*$  for each country by averaging the variable of the net trade over the period between 1976 and 2005. We find that  $\bar{Q}_i^* > 0$  for Japan and  $\bar{Q}_i^* < 0$  for the United States. Therefore, according to the feedback mechanism derived in this work, even without knowing the theoretical models of the internal and external dynamics, we conclude that the macroeconomic system for the United States is a negative feedback system, i.e., the sign of the feedback signal  $R_i(t) = Q_i(t) - \bar{Q}_i^*$  is opposite to that of the fluctuation of GDP  $y_i(t) - y_i^*(t)$ . On the other hand, the macroeconomic system in Japan is a positive feedback system. Such conclusions agree with the real data well, which are shown in Fig. 8.

## VI. SUMMARY AND DISCUSSION

In summary, we proposed a model of complex systems with preferential flow among nodes to study the fluctuation behavior, and derived a feedback mechanism in the model. We illustrated the feedback mechanism in both a macroeconomic network and a city-population network, which demonstrated the effectiveness of the theoretical results. Though our analytical results require a linear internal dynamics of a node, the numerical simulation on the city-population system shows that the feedback mechanism holds near the equilibrium point for a network even with nonlinear internal dynamics.

Furthermore, we verified the feedback mechanism in a complex system with a scale-free topology and found that the mechanism is preserved for hub nodes in such a network. We also study the feedback mechanism in a network with an evolving topology. Two cases of the topology evolving are considered. One considers the effect of the topology noise on the feedback mechanism; the other includes the rewiring dynamics. The feedback mechanism is confirmed in both the two cases.

The feedback mechanism can be used to estimate the strength of the fluctuations of the nodes by calculating the steady net flux of the nodes. More precisely, the feedback mechanism can be used to judge whether the external fluctuation strengthens the internal fluctuation. When the exact mathematical model for a system is not available, the observation data can be utilized to judge whether the system of a node in the network is a positive feedback or a negative feedback system. To evaluate the strength of the fluctuations of a node in the network, we need not the data set of all nodes. We merely need the time series of in-flux, out-flux, and output of the node to be evaluated. Of course, the trends of these data should be estimated.

The scaling properties of the statistic fluctuation behavior in complex systems, the Taylor's law, has been studied in much of the literature [6–12]. The law states that the relationship between the fluctuations and the mean of a system variable can be written as  $\text{fluctuations} \approx \text{const} \times \text{mean}^\gamma$ . Enormous empirical investigations show that  $1/2 \leq \gamma \leq 1$ . Impact inhomogeneity and constituent correlations may be the underlying mechanism for generating the Taylor's law with any value of  $\gamma$  [8]. The feedback mechanism between the external fluctuation and the internal fluctuation in the present paper may be another way to generate the Taylor's law with  $1/2 \leq \gamma \leq 1$ . Consider a simple case of our model that all the nodes in the network are identical. If they are completely disconnected from the network, they have identical averages and fluctuations of the outputs. When they are connected with each other under some kinds of topology, the steady output of each node  $y_i^*$ , or the average output of each node, depends on the steady net flux  $Q_i^*$ . Larger  $Q_i^*$  induces larger  $y_i^*$ . Meanwhile, larger  $Q_i^*$  with  $Q_i^* > 0$  means a stronger positive feedback effect, which causes higher fluctuations. On the other hand, smaller  $Q_i^*$  with  $Q_i^* < 0$  induces smaller  $y_i^*$ , and causes lower fluctuations. In short, the feedback mechanism in the present paper shows that if a node has positive(negative) feedback, then a higher(lower) aver-

age of the output and higher(lower) fluctuations of the output are obtained, which agrees well with the Taylor's law. Further investigation of the relationship between the Taylor's law and the effect of the feedback is a future work.

#### APPENDIX A: DERIVATION OF THE RELATIONSHIP BETWEEN $R_i(t+1)$ AND $y_i(t)$

The effect of the shocks is characterized by a stochastic variable with the normal distribution in the present paper  $\phi_i(t) = \xi_i(t)\alpha_i(t)$  with  $\xi_i(t) \sim N(0,1)$  and  $\alpha_i(t) > 0$ . Since the internal dynamical system of node  $i$ ,  $\mathcal{L}_i$  [Eq. (5)], is a linear system that is asymptotically stable, the impulse response  $h_i(m)$  of the linear system satisfies [15]

$$\lim_{m \rightarrow \infty} h_i(m) = 0. \quad (\text{A1})$$

Suppose that

$$h_i(m) = 0 \quad \text{for } m > M. \quad (\text{A2})$$

Assume that the network dynamics of node  $i$  [Eq. (6)] has initial conditions as  $y_i(t) = y_i^*$  and  $\phi_i(t) = 0$  for  $t \leq 0$ . Then  $R_i(t) = 0$  for  $t \leq 1$ . Thus Eq. (6) can be rewritten as

$$y_i(t) - y_i^* = \sum_{m=\max(1,t-M)}^t [\phi_i(m) + R_i(m)]h_i(t-m), \quad t \geq 1. \quad (\text{A3})$$

Considering that  $R_i(1) = 0$ , we have from Eq. (A3)

$$y_i(1) = y_i^* + \phi_i(1)h_i(0). \quad (\text{A4})$$

Let

$$A_j^* = \frac{1}{N} \sum_{l=1}^N w_{l,j} y_l^* \quad (\text{A5})$$

and

$$A_j(1) = \frac{1}{N} \sum_{l=1}^N w_{l,j} y_l(1), \quad j = 1, 2, \dots, N. \quad (\text{A6})$$

As  $y_l(1)$  conforms to the normal distribution with mean  $y_l^*$  and variance  $[\alpha_l(1)h_l(0)]^2$ ,  $A_j(1)$  conforms to the normal distribution with the mean

$$E[A_j(1)] = A_j^* \quad (\text{A7})$$

and the variance

$$D[A_j(1)] = \frac{1}{N^2} \sum_{l=1}^N [\alpha_l(1)h_l(0)w_{l,j}]^2. \quad (\text{A8})$$

Assume that the number of nodes  $N$  is sufficiently large. Then  $D[A_j(1)]$  converges to 0 and stochastic variable  $A_j(1)$  converges to  $A_j^*$ . According to Eq. (3),

$$Q_i(2) = y_i(1) \left[ \sum_{j=1}^N \frac{y_j(1)k_j}{NA_j^*} w_{i,j} - k_i \right]. \quad (\text{A9})$$

Since  $N$  is sufficiently large,

$$Q_i(2) \approx y_i(1) \left[ \sum_{j=1}^N \frac{y_j(1)k_j}{NA_j^*} w_{i,j} - k_i \right]. \quad (\text{A10})$$

As with stochastic variable  $A_j(1)$ , stochastic variable  $\sum_{j=1}^N \frac{y_j(1)k_j}{NA_j^*} w_{i,j}$  converges to its mean

$$B_i^* = E \left( \sum_{j=1}^N \frac{y_j(1)k_j}{NA_j^*} w_{i,j} \right) = \sum_{j=1}^N \frac{y_j^* k_j}{NA_j^*} w_{i,j}. \quad (\text{A11})$$

Therefore,

$$Q_i(2) \approx y_i(1)[B_i^* - k_i]. \quad (\text{A12})$$

According to Eq. (4),

$$Q_i^* = y_i^*[B_i^* - k_i]. \quad (\text{A13})$$

Thus, according to  $R_i(t) = Q_i(t) - Q_i^*$ ,

$$\begin{aligned} R_i(2) &= Q_i(2) - Q_i^* \approx [y_i(1) - y_i^*](B_i^* - k_i) \\ &= [y_i(1) - y_i^*]Q_i^*/y_i^*. \end{aligned} \quad (\text{A14})$$

From Eq. (A3),

$$y_i(2) = y_i^* + [R_i(2) + \phi_i(2)]h_i(0) + \phi_i(1)h_i(1). \quad (\text{A15})$$

According to Eqs. (A14) and (A15), both  $R_i(2)$  and  $y_i(2)$  are stochastic variables with the normal distribution. Let

$$A_j(2) = \frac{1}{N} \sum_{l=1}^N w_{l,j} y_l(2). \quad (\text{A16})$$

Taking into account of Eq. (A15), like stochastic variable  $A_j(1)$ , stochastic variable  $A_j(2)$  converges to

$$E[A_j(2)] = A_j^*. \quad (\text{A17})$$

Similar to the stochastic variable  $\sum_{j=1}^N \frac{y_j(1)k_j}{NA_j^*} w_{i,j}$ , stochastic variable  $\sum_{j=1}^N \frac{y_j(2)k_j}{NA_j^*} w_{i,j}$  converges to  $B_i^*$ . Therefore,

$$Q_i(3) = y_i(2)[B_i^* - k_i]. \quad (\text{A18})$$

Thus,

$$\begin{aligned} R_i(3) &= Q_i(3) - Q_i^* \approx (y_i(2) - y_i^*)(B_i^* - k_i) \\ &= (y_i(2) - y_i^*)Q_i^*/y_i^*. \end{aligned} \quad (\text{A19})$$

By a similar calculation from Eqs. (A15)–(A19), we have

$$\begin{aligned} y_i(t) &= y_i^* + \sum_{m=\max(1,t-M)}^t h_i(t-m) \{ [y_i(m-1) - y_i^*]Q_i^*/y_i^* \\ &\quad + \phi_i(m) \}, \end{aligned} \quad (\text{A20})$$

$$R_i(t+1) = [y_i(t) - y_i^*]Q_i^*/y_i^*, \quad (\text{A21})$$

where  $t=3, 4, \dots$

**APPENDIX B: RELATIONSHIP BETWEEN  $R_i(t+1)$   
AND  $y_i(t)$  IN A NETWORK WITH AN EVOLVING  
TOPOLOGY**

Assume that the topology evolution is described by  $w_{i,j}(t) = w_{i,j}(0) + \xi_{i,j}(t)\beta_{i,j}(t)$  with  $\xi_{i,j}(t) \sim N(0,1)$  and  $\beta_{i,j}(t) > 0$ . By following the same procedure in Appendix A, in which  $y_i^*$ ,  $Q_i^*$ , and  $w_{i,j}$  are replaced by  $y_i^*(0)$ ,  $Q_i^*(0)$ , and  $w_{i,j}(t)$ , respectively, we will have

$$R_i(t+1) = [y_i(t) - y_i^*(0)]Q_i^*(0)/y_i^*(0), \quad (\text{B1})$$

where  $t = 1, 2, 3, \dots$

Nevertheless, as  $w_{i,j}(t)$  is presently a stochastic variable, the dealing with  $w_{i,j}(t)$  in the corresponding equations needs to be clarified. Equations (A5)–(A8) are taken as examples for the dealing with  $w_{i,j}(t)$ .

We rewrite Eqs. (A5) and (A6) as

$$A_j^* = \frac{1}{N} \sum_{l=1}^N w_{l,j}(0)y_l^*(0) \quad (\text{B2})$$

and

$$A_j(1) = \frac{1}{N} \sum_{l=1}^N w_{l,j}(1)y_l(1), \quad (\text{B3})$$

respectively. As  $y_l(1)$  conforms to the normal distribution with mean  $y_l^*(0)$ , and  $w_{l,j}(1)$  conforms to the normal distribution with mean  $w_{l,j}(0)$  as well,  $A_j(1)$  conforms to the normal distribution with the following mean:

$$E[A_j(1)] = A_j^*. \quad (\text{B4})$$

Let  $\sigma_l^2$  be the variance of the stochastic variable  $w_{l,j}(1)y_l(1)$ . As  $y_l(1)$  has the variance  $[\alpha_l(1)h_l(0)]^2$  and  $w_{l,j}(1)$  has the variance  $[\beta_{l,j}(1)]^2$ , there exists a real number  $M_l$ ,  $\sigma_l < M_l$ . Then,

$$D[A_j(1)] < \frac{1}{N^2} \sum_{l=1}^N (M_l)^2. \quad (\text{B5})$$

Assume that the number of nodes  $N$  is sufficiently large. Then  $D[A_j(1)]$  converges to 0 and stochastic variable  $A_j(1)$  converges to  $A_j^*$ .

- 
- [1] S. H. Strogatz, *Nature (London)* **410**, 268 (2001).  
 [2] A. T. Winfree, *The Geometry of Biological Time* (Springer-Verlag, New York, 1990).  
 [3] S. H. Strogatz, *Sync: The Emerging Science of Spontaneous Order* (Hyperion, New York, 2003).  
 [4] S. C. Manrubia, A. S. Mikhailov, and D. H. Zanette, *Emergence of Dynamical Order: Synchronization Phenomena in Complex Systems* (World Scientific, Singapore, 2004).  
 [5] A. Arenas, A. D. Guilerá, J. Kurths, Y. Moreno, and C. Zhou, *Phys. Rep.* **469**, 93 (2008).  
 [6] M. A. de Menezes and A. L. Barabási, *Phys. Rev. Lett.* **93**, 068701 (2004).  
 [7] Z. Eisler and J. Kertész, *Phys. Rev. E* **73**, 046109 (2006).  
 [8] Z. Eisler, I. Bartos, and J. Kertész, *Adv. Phys.* **57**, 89 (2008).  
 [9] M. A. de Menezes and A. L. Barabási, *Phys. Rev. Lett.* **92**, 028701 (2004).  
 [10] J. Duch and A. Arenas, *Phys. Rev. Lett.* **96**, 218702 (2006).  
 [11] S. Yoon, S. H. Yook, and Y. Kim, *Phys. Rev. E* **76**, 056104 (2007).  
 [12] S. Meloni, J. Gomez-Gardenes, V. Latora, and Y. Moreno, *Phys. Rev. Lett.* **100**, 208701 (2008).  
 [13] P. J. Antsaklis and A. N. Michel, *Linear Systems* (Springer, Berlin, 2006).  
 [14] A. Arenas, A. Díaz-Guilera, and R. Guimerà, *Phys. Rev. Lett.* **86**, 3196 (2001).  
 [15] W. S. Levine, *The Control Handbook* (CRC, Boca Raton, FL, 1996).  
 [16] P. Samuelson, *Rev. Econ. Stat.* **21**, 75 (1939).  
 [17] H. Fan, Z. Wang, and K. Aihara, *Math. Eng. Tech. Rep.* **60**, 1 (2007).  
 [18] A. L. Barabási and R. Albert, *Science* **286**, 509 (1999).  
 [19] Y. P. Jeon and B. J. McCoy, *Phys. Rev. E* **72**, 037104 (2005).  
 [20] S. N. Dorogovtsev and J. F. F. Mendes, *Evolution of Networks: From Biological Nets to the Internet and WWW* (Oxford University, Oxford, 2003).  
 [21] T. S. Evans and A. D. K. Plato, *Phys. Rev. E* **75**, 056101 (2007).  
 [22] H. Fan, Z. Wang, T. Ohnishi, H. Saito, and K. Aihara, *Phys. Rev. E* **78**, 026103 (2008).  
 [23] Even if the dynamics of one node is nonlinear in real-world networks, the theory of local dynamics around any equilibrium in a nonlinear system relies on a solid understanding of linear dynamics.  
 [24] The internal dynamics of a city is perhaps more complex than the logistic map. The complexity of internal dynamics does not influence the result that the feedback mechanism holds around the equilibrium point.  
 [25] Data available at <http://earthtrends.wri.org>